



Supplement of

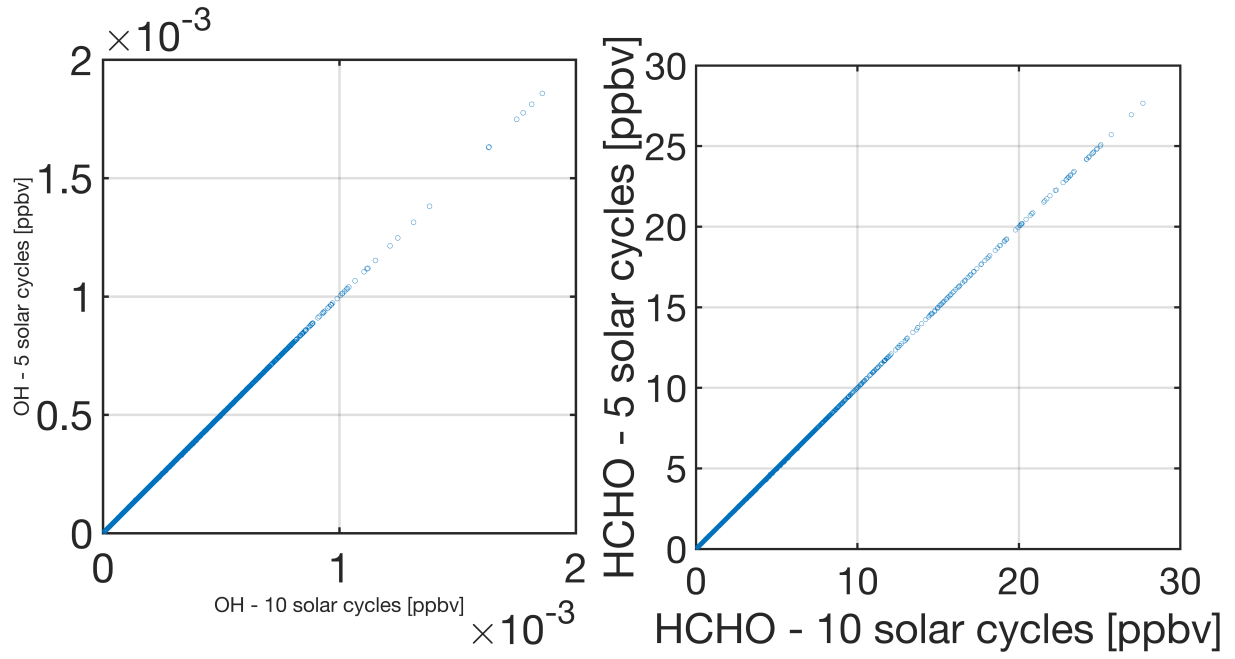
Characterization of errors in satellite-based HCHO / NO₂ tropospheric column ratios with respect to chemistry, column-to-PBL translation, spatial representation, and retrieval uncertainties

Amir H. Souri et al.

Correspondence to: Amir H. Souri (a.souri@nasa.gov, amir.souri@morgan.edu)

The copyright of individual parts of the supplement might differ from the article licence.

1 **Supplementary materials:**



2 **Figure S1.** The comparison of simulated HCHO (left) and OH (right) with 5 (y-axis) and 10 (x-axis)
3 solar cycles.
4
5

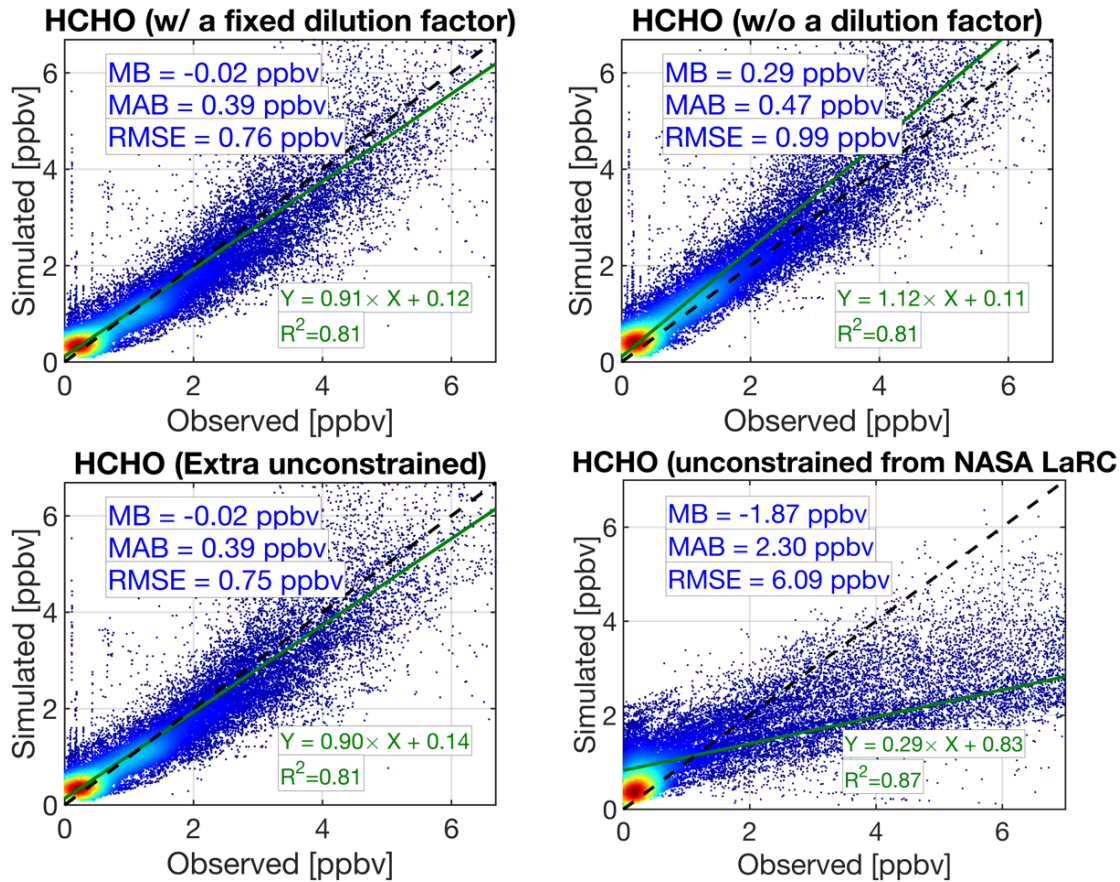
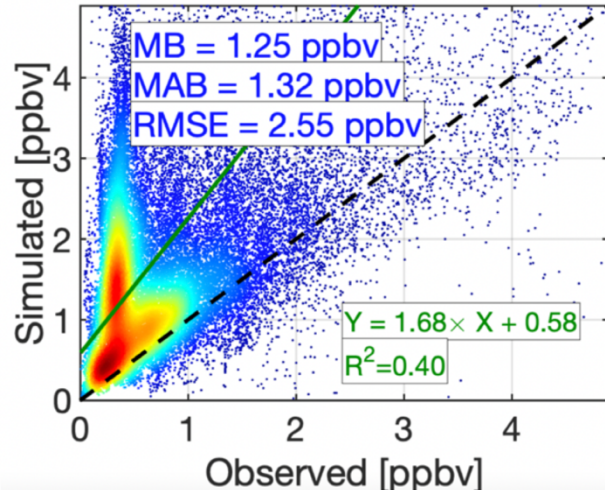
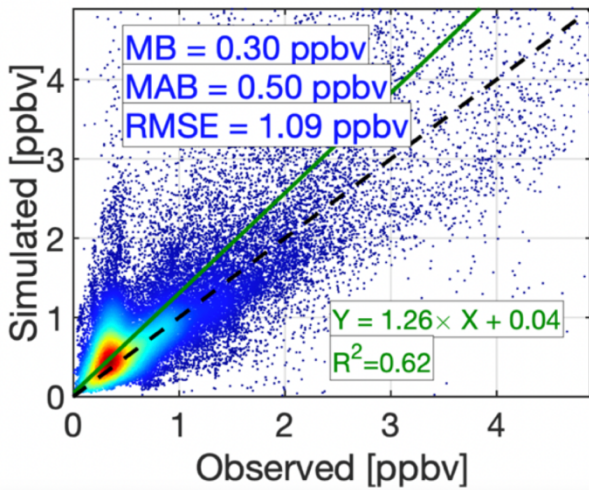
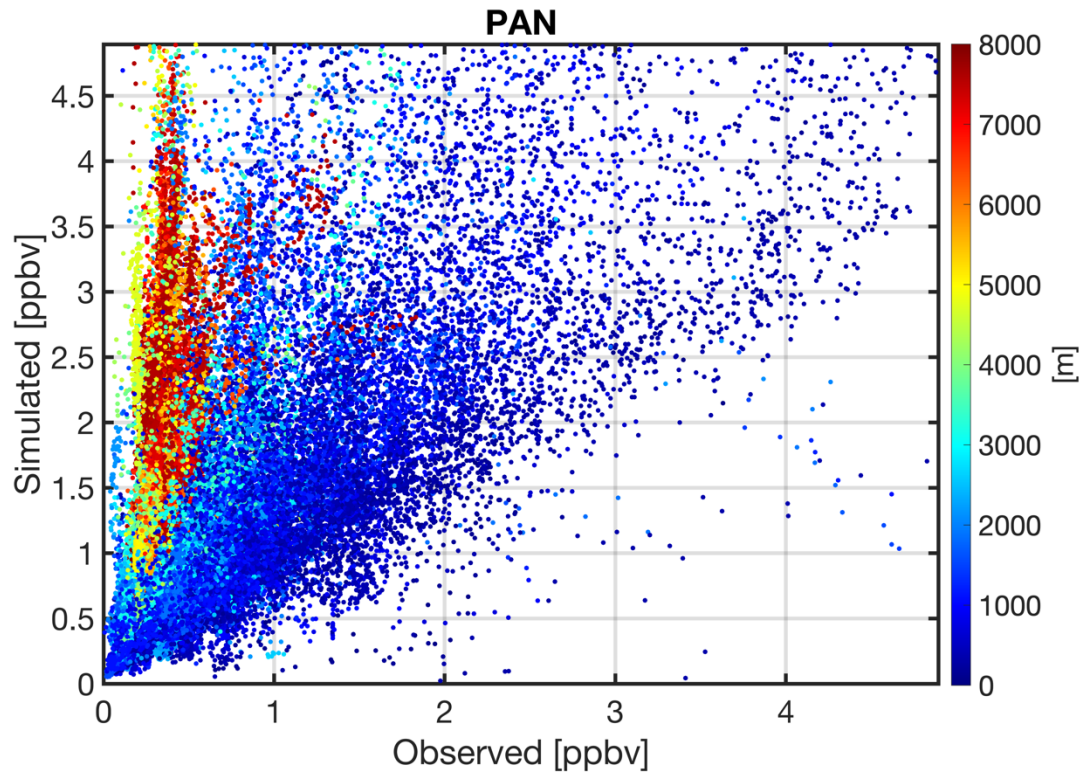


Figure S2. The comparison of simulated HCHO mixing ratios compared to observations for (top left) our F0AM setup with the dilution process on, (top right) the same model but without the dilution process, (bottom left) our F0AM setup with dilution process on and without constraining HNO₃ and H₂O₂, and (bottom right) NASA LaRC unconstrained model based on Schroeder et al. (2021). All points are based on a 10-sec sampling size.



14
15
16
17

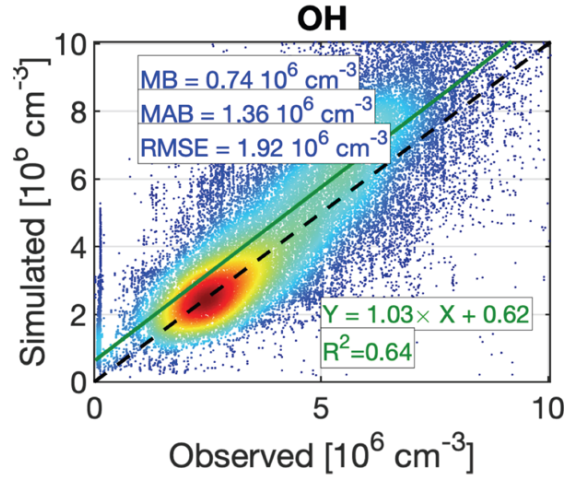
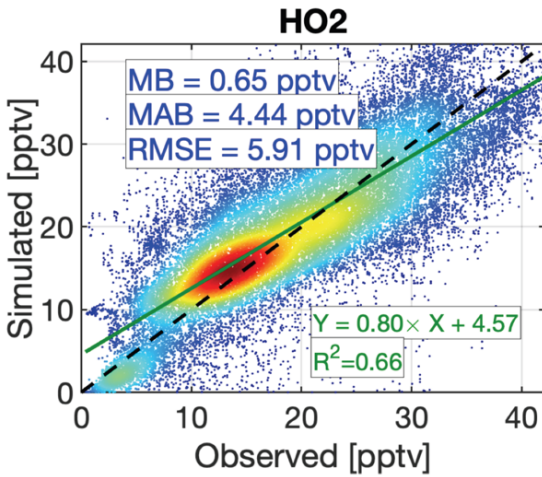
Figure S3. (left) The comparison of PAN mixing ratios w/ a fixed dilution factor and (right) w/o a dilution factor during the KORUS-AQ campaign.



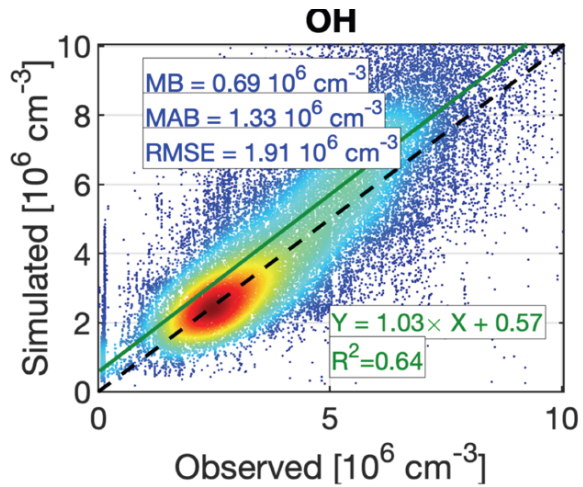
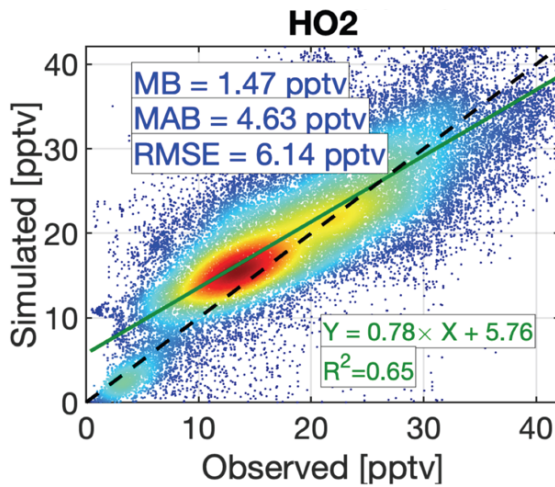
18
19

Figure S4. Same as the right panel in Figure S3 but with aircraft altitude superimposed.

20



21



22

23

Figure S5. (top) The simulation of OH and HO₂ using a fixed dilution factor during the KORUS-AQ campaign. (bottom) without considering the dilution factor.

24

25

26

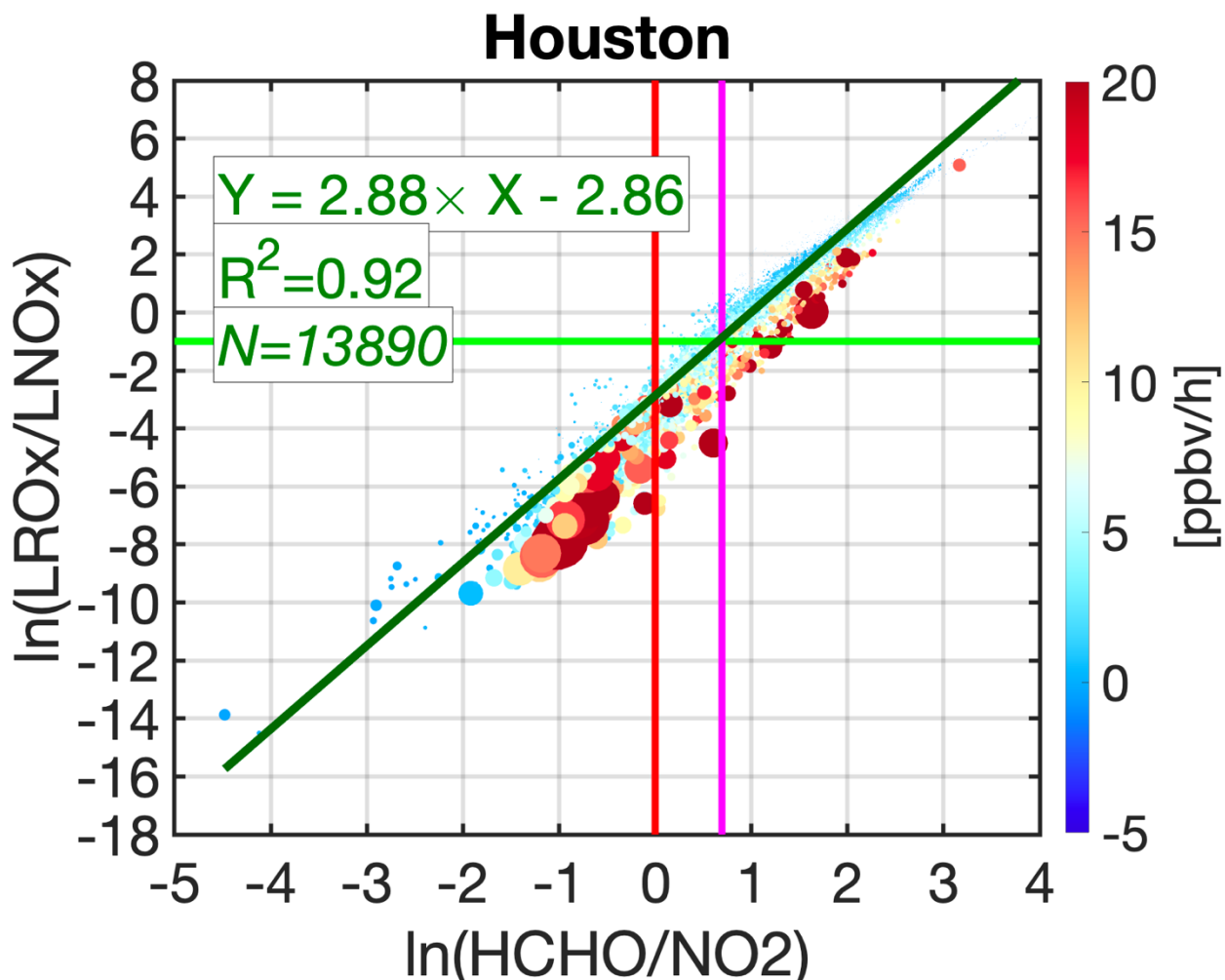
27

28

29

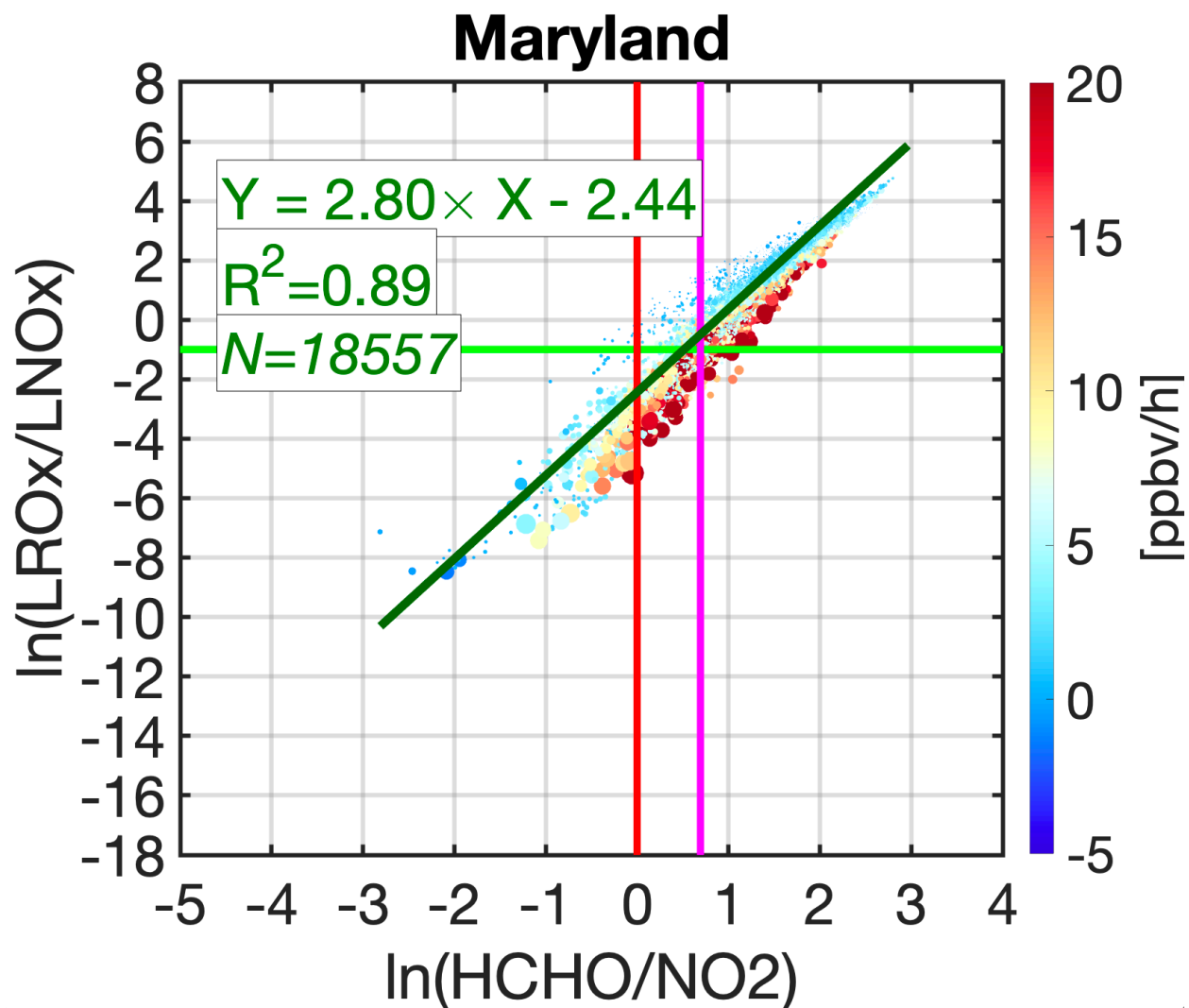
30

31



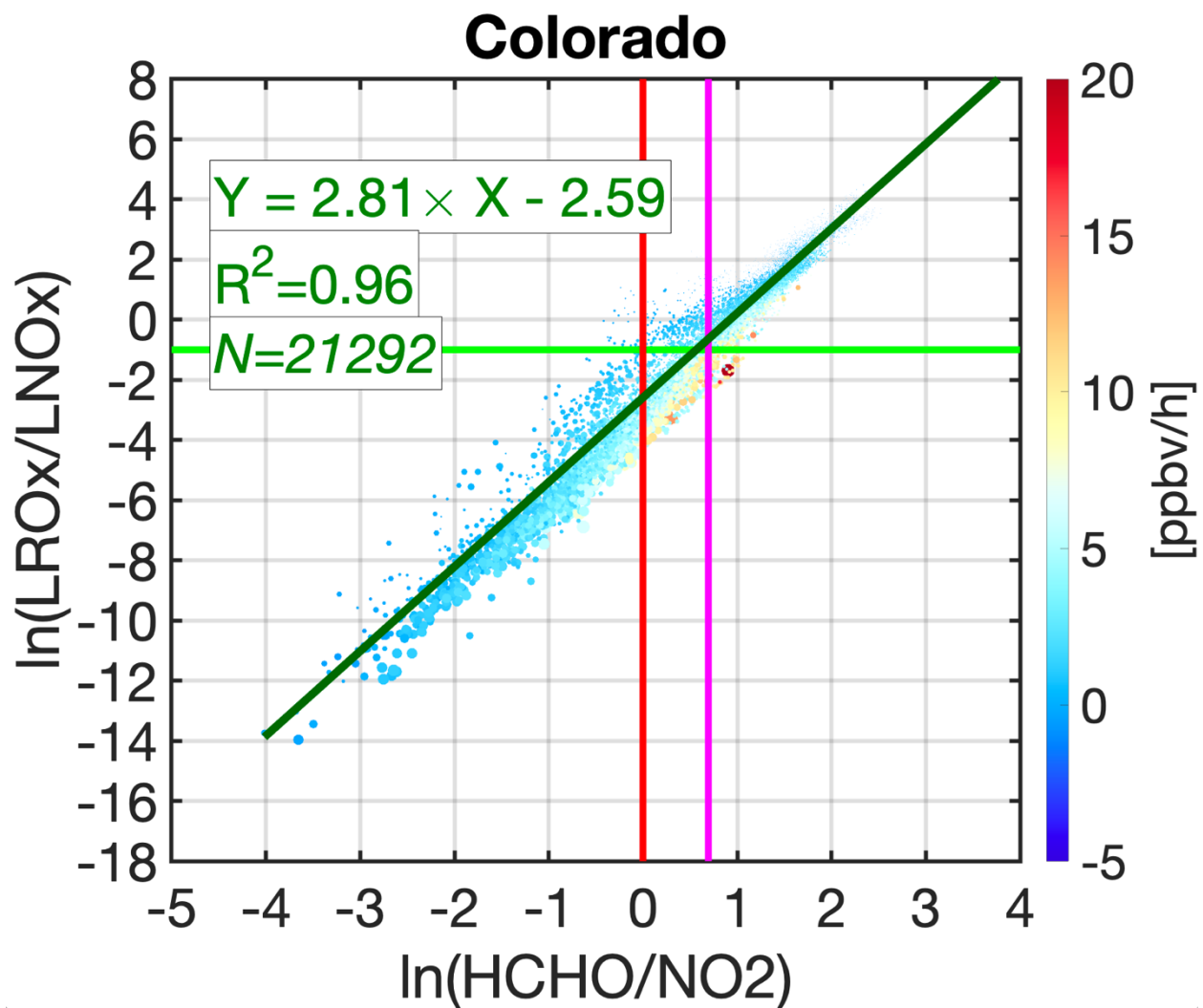
32
 33
 34
 35
 36
 37
 38
 39
 40
 41

Figure S6. The scatterplot of natural logarithm-transformed of HCHO/NO₂ versus LROx/LNO_x based on the simulated values performed by the F0AM box model during DISCOVER-AQ Texas 2013. The heat color indicates the calculated ozone production rates (PO₃). The size of each data point is proportional to HCHO×NO₂. The light green line is the baseline separator of NO_x-sensitive (above the line) and VOC-sensitive (below the line) regimes. We overlay HCHO/NO₂=1 and HCHO/NO₂=2 as red and purple lines, respectively. The dark green line indicates the least-squares fit to the paired data.



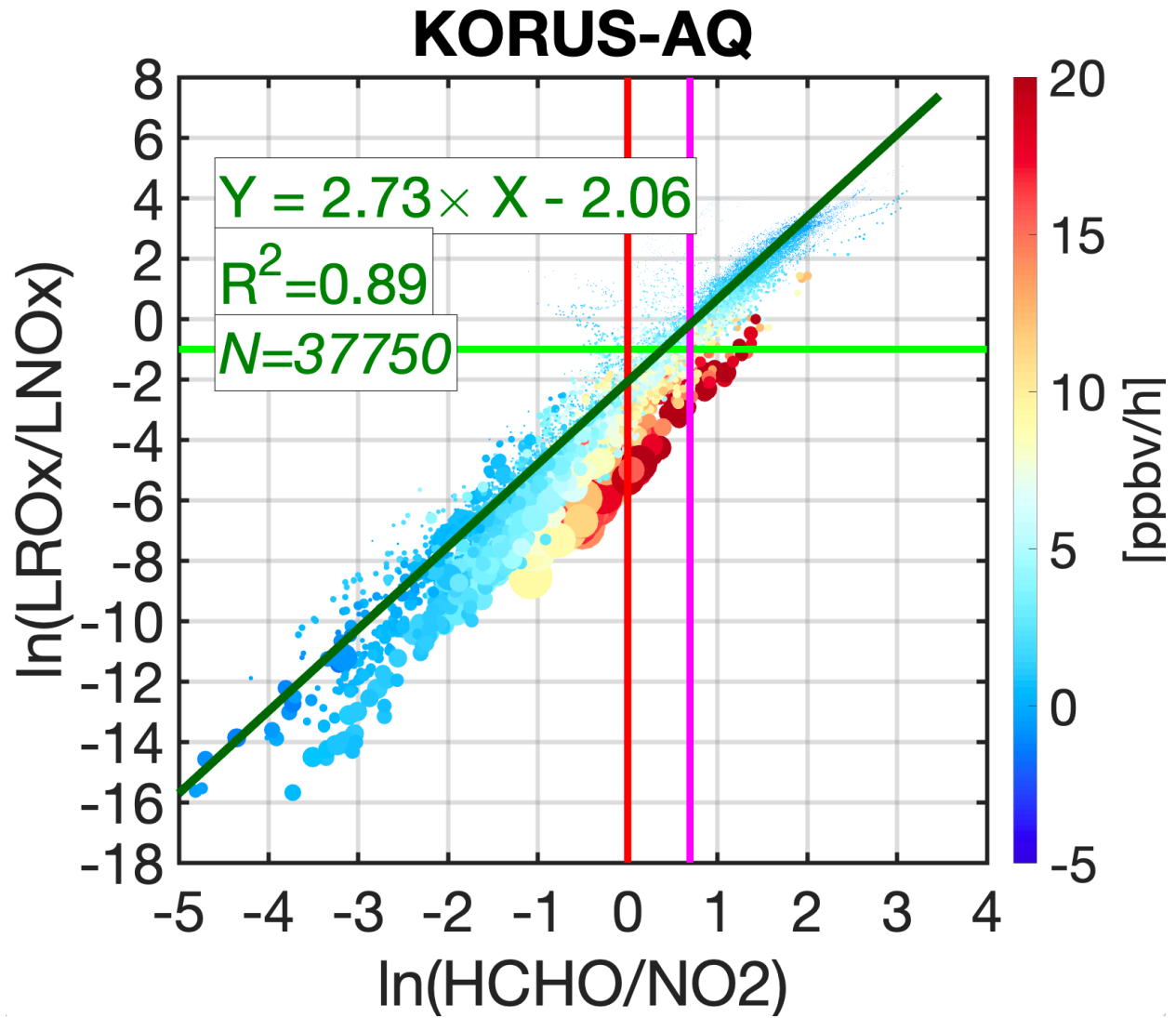
42
43
44

Figure S7. Same as Figure S6 but for DISCOVER Maryland 2011.



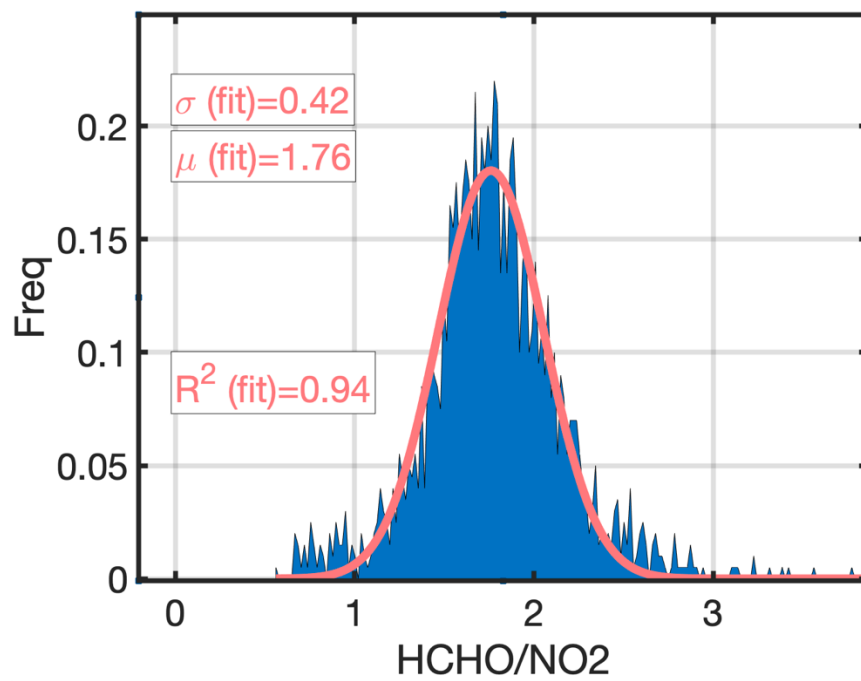
45
46
47

Figure S8. Same as Figure S6 but for DISCOVER Colorado 2014.

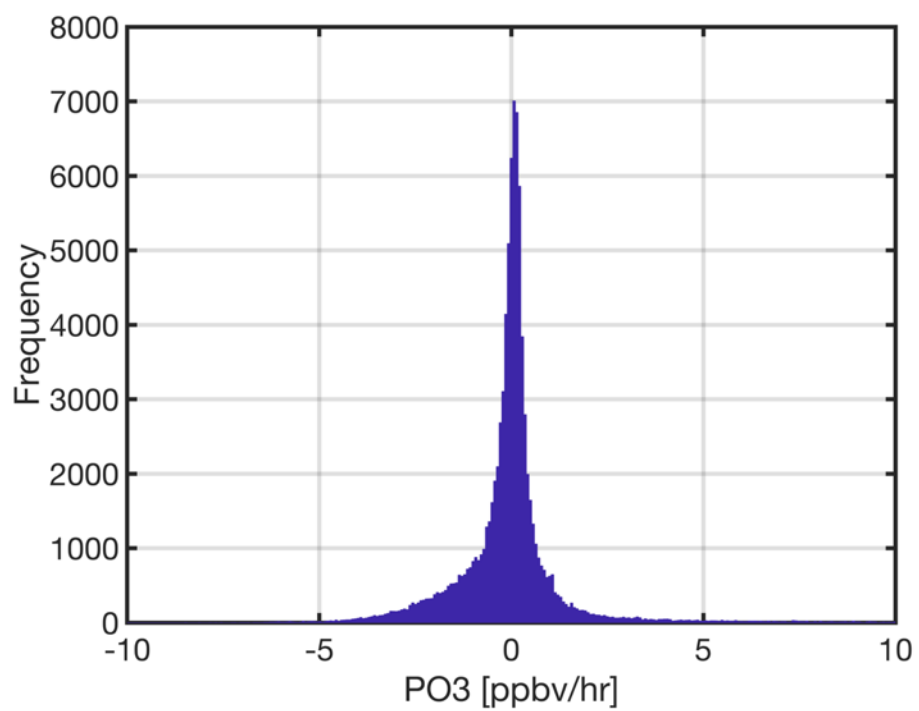


48
49
50

Figure S9. Same as Figure S6 but for KORUS-AQ 2016.

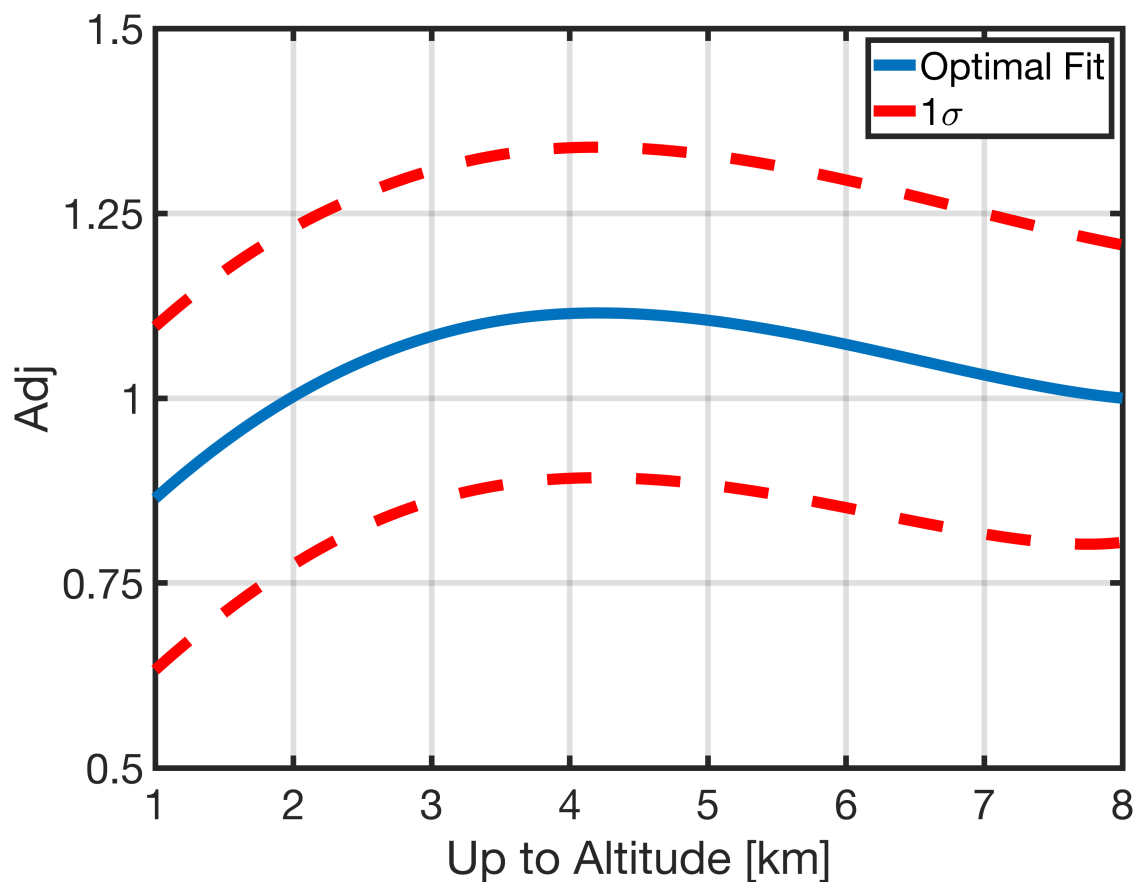


51
52 **Figure S10.** The histogram of transitioning ratios based on simulated values of $\ln(\text{LROx/LNOx})$
53 = -1.0 ± 0.2 .
54

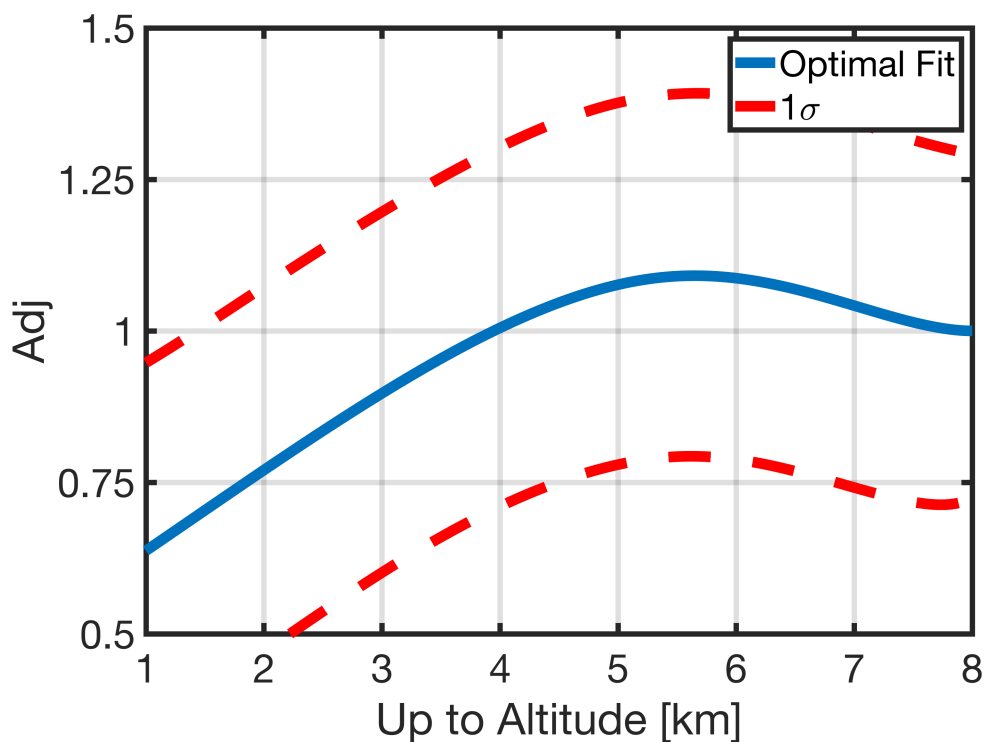


55
56
57

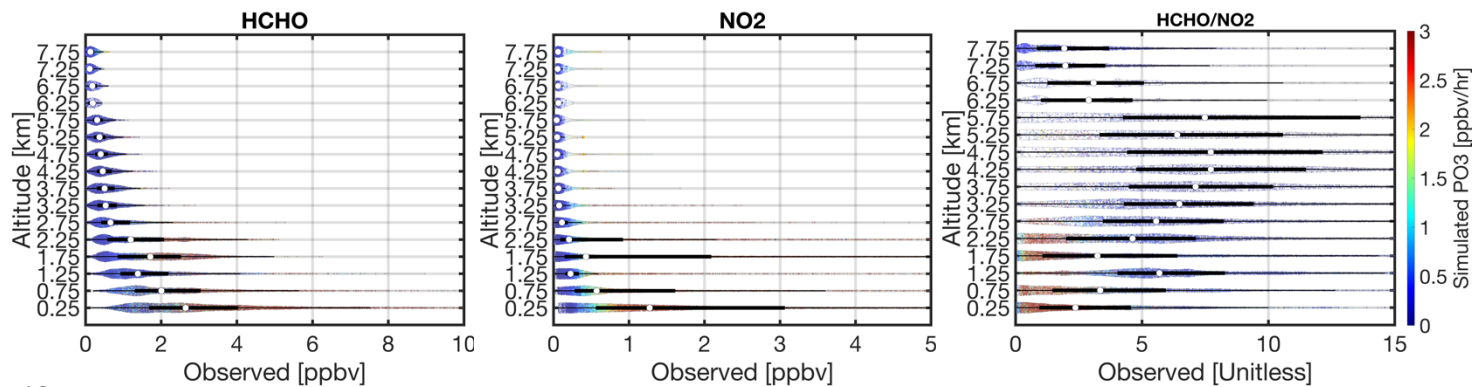
Figure S11. The residuals for the fit described in Eq4 in the main text.



59
 60 **Figure S12.** The adjustment factor defined as the ratio of the centroid of the polygon bounding 1st
 61 and 75th percentiles of the observed HCHO/NO₂ columns by the NASA aircraft between the surface
 62 to 8 km to the ones between the surface and the desired altitude. This factor can be easily applied
 63 to the observed HCHO/NO₂ columns to translate the value to the desired altitude stretching down
 64 to the surface (i.e., PBLH). Only afternoon observations are used.
 65

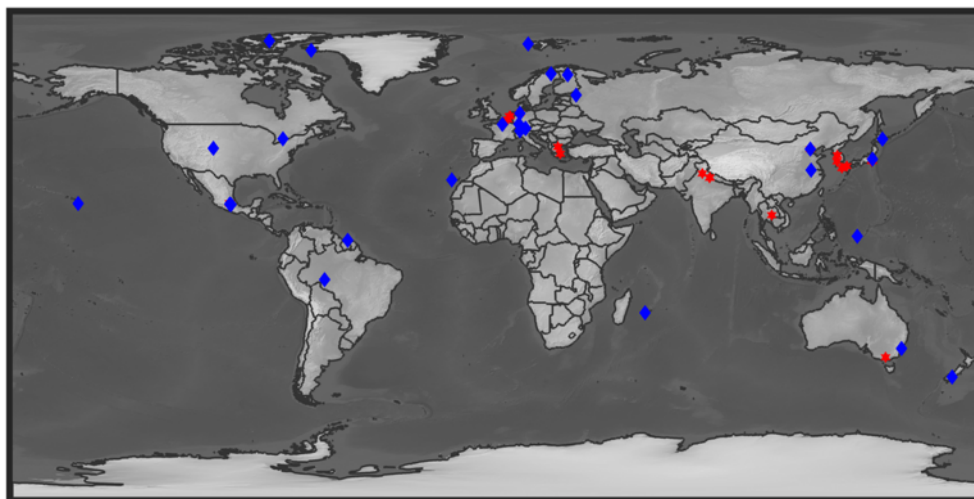


66
 67 **Figure S13.** The adjustment factor defined as the ratio of the centroid of the polygon bounding 25th
 68 and 75th percentiles of the observed HCHO/NO₂ columns by the NASA's aircraft between the
 69 surface to 8 km to the ones between the surface and a desired altitude. This factor can be easily
 70 applied to the observed HCHO/NO₂ columns to translate the value to a desired altitude stretching
 71 down to the surface (i.e., PBLH). Only observations made during morning are used.
 72



74
 75 **Figure S14.** The violin plots of the morning vertical distribution of HCHO, NO₂, and
 76 HCHO/NO₂ observations were collected during DISCOVER-AQ Texas, Colorado, Maryland,
 77 and KORUS-AQ campaigns. The violin plots demonstrate the data distribution (i.e., a wider
 78 width means a higher frequency). White dots show the median. A solid black line shows both the
 79 25th and 75th percentiles. The heatmap denotes the simulated ozone production rates.
 80
 81

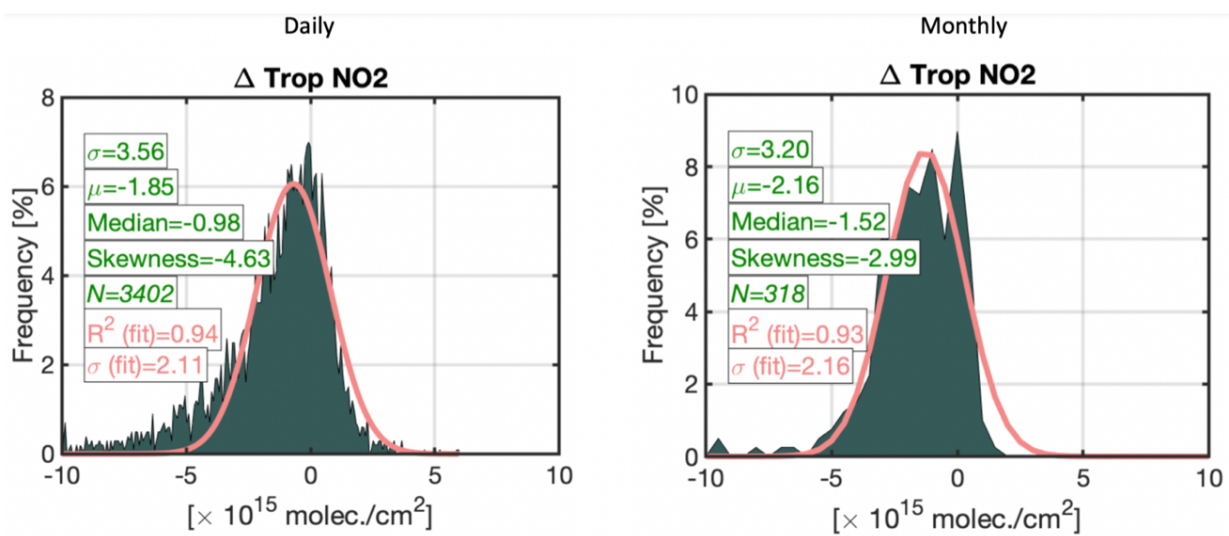
82



83
84
85

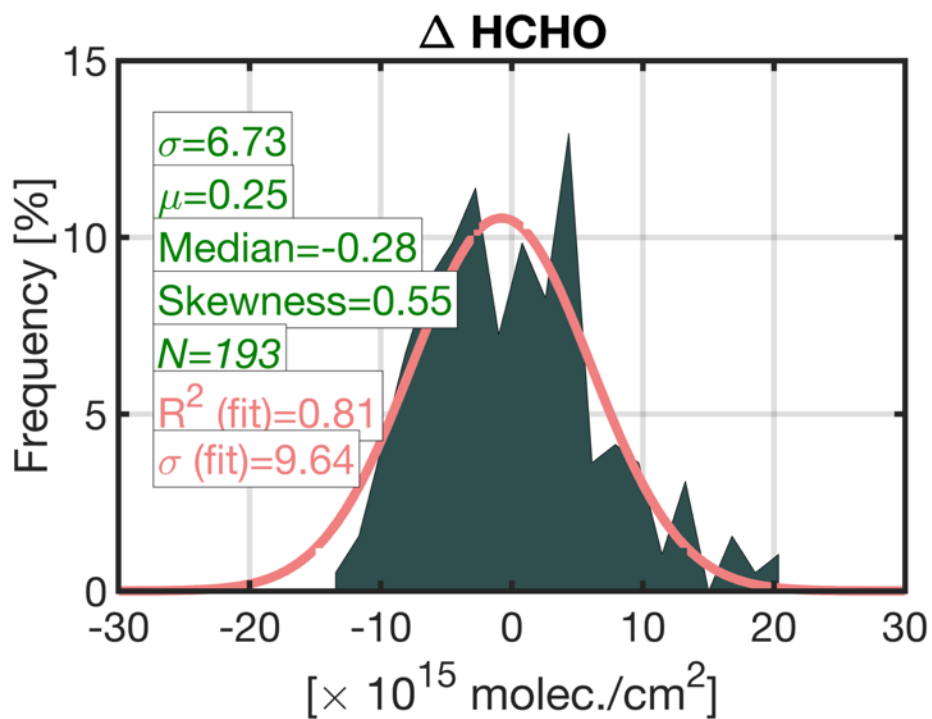
Figure S15. The location map of MAX-DOAS (red) and FTIR (blue) stations.

86

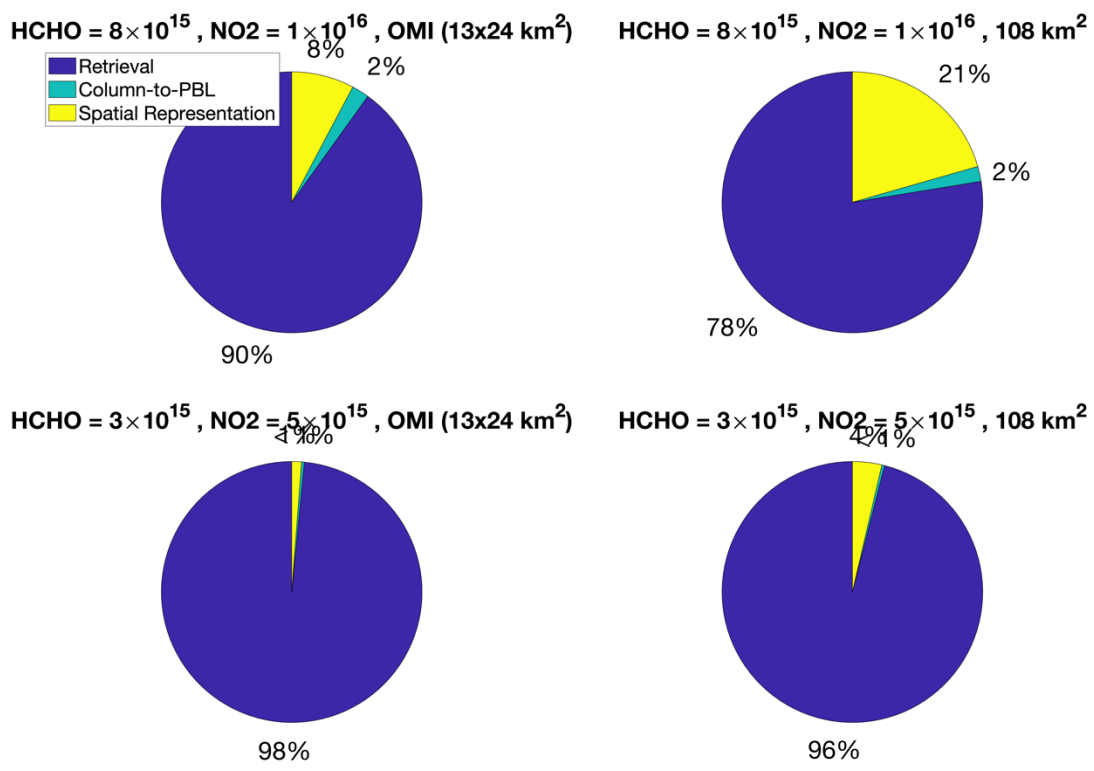


87
88
89
90

Figure S16. Same as Figure 10 in the main manuscript but on (left) daily and (right) monthly basis.



91
 92 **Figure S17.** The histogram of the differences between OMI and corrected GEOS-Chem
 93 simulations on monthly basis. The statistics in green color are based on all data, whereas those in
 94 pink are based on the fitted Gaussian function.
 95



96
 97 **Figure S18.** The fractional errors of retrieval (blue), column to PBL translation (green), and spatial
 98 representation (yellow) of the total error budget for different concentrations and footprints based
 99 on OMI sigma values. HCHO OMI sigma is from a monthly comparison (Figure S17).
 100